Accepted Manuscript

Uricase-free on-demand colorimetric biosensing of uric acid enabled by integrated CoP nanosheet arrays as a monolithic peroxidase mimic

Yanfang He, Fei Qi, Xiangheng Niu, Wenchi Zhang, Xifeng Zhang, Jianming Pan

PII: S0003-2670(18)30355-6

DOI: 10.1016/j.aca.2018.02.073

Reference: ACA 235789

To appear in: *Analytica Chimica Acta*

Received Date: 26 September 2017

Revised Date: 2 February 2018

Accepted Date: 27 February 2018

Please cite this article as: Y. He, F. Qi, X. Niu, W. Zhang, X. Zhang, J. Pan, Uricase-free on-demand colorimetric biosensing of uric acid enabled by integrated CoP nanosheet arrays as a monolithic peroxidase mimic, *Analytica Chimica Acta* (2018), doi: 10.1016/j.aca.2018.02.073.

Uricase-free on-demand colorimetric biosensing of uric acid enabled by integrated CoP nanosheet arrays as a monolithic peroxidase mimic

Yanfang He, Fei Qi, Xiangheng Niu,* Wenchi Zhang, Xifeng Zhang, Jianming Pan*

Institute of Green Chemistry and Chemical Technology, School of Chemistry and Chemical Engineering, Jiangsu University, Zhenjiang 212013, China

* Corresponding authors. E-mail: niuxiangheng@126.com; (X.H. Niu) jmpan@ujs.edu.cn (J.M. Pan)

Abstract: In clinical diagnosis, monitoring of uric acid (UA) is generally realized by combining uricase with natural peroxidase. The use of bio-enzymes, however, shadows some highlights of these methods due to their vulnerable activities against environments. Herein, we report a novel biosensor for the natural enzyme-free colorimetric detection of UA by using CoP nanosheet arrays grown on Ni foam (NF) as a monolithic peroxidase mimic. The integrated nanozyme can be put into and taken out from reaction systems conveniently with only tweezers, making it possible for on-demand analysis. As demonstrated, the obtained CoP/NF exhibits outstanding peroxidase-like activity to trigger the oxidation reaction of colorless 3,3'5,5'-tetramethylbenzidine (TMB) to a blue product (TMBox) mediated by H_2O_2. It is found that the blue TMBox can be reduced to colorless TMB again by UA selectively, thus the presence of UA in solutions will suppress the color reaction of TMB. Based on this principle, an uricase-free biosensor is developed for the photometric determination of UA, providing a wide detection range of 1~200 μM and a limit of detection down to 1.0 μM. In addition, the fabricated biosensor can be applied for measuring UA in clinical samples with merits of simple operation and good reliability, exhibiting its great promise in clinical diagnosis.

Keywords: Monolithic nanozyme; On-demand analysis; UA; Natural enzyme-free; Colorimetric detection

1. Introduction

Uric acid (UA) is a final product of the purine metabolism process in human body. However, the abnormal UA level in body fluids can cause a series of diseases including arthritis, urolithiasis and Lesch-Nyhan syndrome [1-3]. In addition, the UA level is also an important indicator for pneumonia and leukemia [4]. Therefore, efficient detection of UA in serum and urine has turned to be a significant means for disease prevention and diagnosis.

In clinical practice, detection of UA is generally achieved via the combination of uricase with natural peroxidase [5, 6].The uricase first catalyzes UA into allantoin, simultaneously producing the H_2O_2 intermedium, which is then catalyzed by the natural peroxidase and detected electrochemically or optically [7-10]. This uricase-peroxidase coupling method provides excellent selectivity and sensitivity for UA monitoring. However, the use of natural enzymes shadows some highlights of the method, because the two bio-enzymes used are very sensitive to surroundings (pH, temperature, chemical reagents, etc.) and their vulnerable activities may result in the poor stability, repeatability and storability of biosensors.

In recent years, a few nanomaterials with enzyme-like characteristics (nanozymes) have been explored as an alternative of natural peroxidase, oxidase or superoxide dismutase [11-16]. In comparison with traditional bio-enzymes, nanozymes exhibit significantly enhanced stability against harsh environments [17, 18]. In addition, it is relatively easy to utilize advanced nanotechnologies to massively prepare nanozymes and skillfully tailor their properties at low cost. With these advantages, nanozymes are

playing important roles in chemical, analytical and biomedical applications [12, 17, 19]. On this occasion, Lu and co-workers developed the metal-organic framework MIL-53(Fe) as a peroxidase mimic and incorporated it with uricase to realize the colorimetric detection of UA [20]. Subsequently, $ZnFe_2O_4$ particles [21], CoSe nanocrystals [22] and Cu^{2+} [23] were also employed as mimetic peroxidases for UA biosensing. Among these developed methods, although the explored nanozymes can play the role of peroxidase, the natural uricase is still required for UA detection. Hence, the common shortcomings of an enzyme-based biosensor, as mentioned above, still leave significant room for improvement.

Herein, we report an integrated nanozyme-based assay for the colorimetric detection of UA with no use of any natural enzyme. For the first time, CoP nanosheet arrays grown on Ni foam (NF) were fabricated as a monolithic peroxidase mimic, which exhibits outstanding peroxidase-like activity to trigger the oxidation reaction of colorless 3,3'5,5'-tetramethylbenzidine (TMB) to a blue species (TMBox) in the presence of H_2O_2. It was found that the blue TMBox can be reduced to colorless TMB again by UA selectively, so the presence of UA in solutions can suppress the color reaction of TMB. On the basis of this principle, the UA level can be detected by measuring the absorbance decrease of TMBox. The main novelty of our assay is concluded as follows: (1) unlike previous bi-enzyme or single-enzyme biosensors, the proposed assay works based on the suppression of the color reaction of TMB (which easily occurs in the presence of the CoP/NF peroxidase mimic and H_2O_2) by UA specifically. More importantly, neither uricase nor natural peroxidase is required. This

characteristic endows the developed assay with excellent stability and repeatability in practical use; (2) also unlike previously reported peroxidase mimics that are dispersed in solutions [24], the active CoP nanosheet arrays are integrated on a bulk support (Ni foam). The resulting monolithic nanozyme can be put into and taken out from reaction systems conveniently with only tweezers, and the catalytic reaction can be stopped and reinstated optionally, making it possible for on-demand analysis. This is different from previously reported dispersed nanozymes in solutions, in which complicated centrifugation or magnetic separation is required after use. This character in our sensor also avoids the use of strong acid like H_2SO_4 as a reaction termination agent. Based on these advantages, enzyme-free colorimetric detection of UA in body fluids can be realized by our integrated nanozyme-based assay.

2.Experimental

2.1. Materials and chemicals

NF (99.8% in purity, 0.5 mm in thickness and 97.2% in porosity) was purchased from Changsha Liyuan New Materials Co., Ltd. $CoSO_4 \cdot 7H_2O$, urea, sodium acetate (NaAc), acetic acid (HAc), TMB, H_2O_2, UA, ascorbic acid (AA), glucose (Glu), cholesterol (Chol) and triglyceride (Trig) were obtained from Sinopharm Chemical Regent Co., Ltd. NaH_2PO_2 was provided by Shanghai Macklin Biochemical Co., Ltd. All other chemicals were of analytical grade and directly used as received. Deionized water was utilized throughout this research.

2.2. Fabrication of the CoP/NF peroxidase mimic

Prior to preparation, the NF substrate was pretreated according to our previous

report [25]. The CoP/NF peroxidase mimic was fabricated via a two-step procedure. First, a hydrothermal synthesis process was carried out to grow $Co(OH)_2$ nanosheet arrays on the NF substrate. To be specific, 1.41 g $CoSO_4 \cdot 7H_2O$ and 1.90 g urea were dissolved in 30 mL deionized water with a mild stir for 20 min; the mixture and a piece of 1 cm×1 cm treated NF were transferred to a 50 mL Teflon-lined stainless steel autoclave for reaction at 120□ for 48 h; after reaction, the formed $Co(OH)_2$/NF was sequentially rinsed with ethanol and deionized water several times and dried in a vacuum oven at 60□ overnight. Then, a phosphorization process was performed to transfer the prepared $Co(OH)_2$ nanosheets into CoP arrays [26, 27]. In detail, a piece of $Co(OH)_2$/NF and 0.6 g NaH_2PO_2 were placed in two nearby quartz boats (with NaH_2PO_2 in the upstream boat of the furnace tube) and heated at 300□ for 1 h in N_2 atmosphere. After phosphorization, the product was collected for use.

2.3. Characterization of the CoP/NF peroxidase mimic

The morphology of materials was examined by a JEOL-6700F field emission scanning electron microscope (FESEM, JEOL). The surface composition of the CoP/NF product was probed by an ESCALABMK-250Xi X-ray photoelectron spectroscope (XPS, Thermo-Fisher Scientific) with Al Kα radiation as the excitation source. X-ray diffraction (XRD) measurements were conducted on a 6100 diffractometer (Shimadzu) with Cu Kα radiation.

2.4. Colorimetric measurements

All colorimetric measurements were performed on a Cary-8454 UV-Vis spectrophotometer (Agilent Technologies). An 8 mM TMB stock solution was

prepared with ethanol for use. H_2O_2 stock solutions with various concentrations were daily prepared. Unless other states, a piece of 5 mm×5mm (or 1 cm×1 cm) CoP/NF was used as the peroxidase mimic. The time-dependent absorbance changes of different reaction systems were recorded with a certain time interval. The apparent steady-state kinetic measurements were performed by recording the absorbance at 652 nm at a 5 s interval within 1 min.

For UA biosensing, UA stock solutions with various concentrations were first prepared with phosphate buffer (0.1 M, pH 8.5). Then, 480 μL of UA stock solution with a certain concentration, a piece of the CoP/NF nanozyme, 2.32 mL of 0.2 M NaAc-HAc buffer (pH 4.0), 150 μL of 9.8 M H_2O_2 stock solution and 50 mL of 8 mM TMB stock solution were mixed and incubated at 30□ for 35 min. Afterwards, the absorption spectrum was recorded after removing the CoP/NF nanozyme from the reaction solution.

The UA level in human serum and urine (these clinical samples were provided by the Affiliated Hospital of Jiangsu University) was detected by the developed UA biosensor. For each serum sample, we eliminated the protein species in advance via acidizing serum and centrifugation at 12,000 rpm for 30 min. Afterwards, 100 μL of the serum supernate, a piece of the CoP/NF nanozyme, 2.7 mL of 0.2 M NaAc-HAc buffer (pH 4.0), 150 μL of 9.8 M H_2O_2 stock solution and 50 mL of 8 mM TMB stock solution were mixed and incubated under optimized conditions. After 35 min, the absorption spectrum was recorded. For each urine sample, a dilution of 2.67 times with 0.1 M phosphate buffer (pH 8.5) was performed before analysis.

3. Results and discussion

3.1. Preparation and characterization of CoP/NF

(Please insert Figure 1 here)

Figure 1. (A) illustrates the fabrication procedure of CoP/NF; (B), (C) and (D) depicts the SEM images of NF, $Co(OH)_2$/NF and CoP/NF, respectively.

As illustrated in Figure 1(A), the monolithic CoP/NF peroxidase mimic is fabricated by combining a hydrothermal synthesis with a phosphorization treatment. The two processes are performed with no complicated operation, and they have been widely used to synthesize phosphide nanostructures [28-30]. In the present study, we employed the SEM technique to inspect the fabrication procedure. As shown in Figure 1(B), the NF substrate exhibits a clean and smooth surface with no material/structure on it. After the hydrothermal synthesis process, a layer of $Co(OH)_2$ nanosheets is grown on the NF surface (C). These interconnected sheets have a thickness of several nanometers, providing a larger surface compared to NF. After phosphorization, it is found that the formed CoP nanosheets are well arrayed on the NF surface (D). Besides, there are a large number of nanoparticles covering the surface of these nanosheets. This architecture mainly originates from the dehydration of $Co(OH)_2$ nanosheets and the subsequent phosphorization under high temperature. The SEM proof demonstrates that CoP nanosheet arrays have been integrated on NF.

To further confirm the composition of CoP/NF, the XRD pattern of CoP/NF is depicted in Figure S1 (Supporting Information). The phosphide product (diffraction peaks of Ni foam are marked with asterisks) provides weak but recognizable

diffraction peaks corresponding to the orthorhombic CoP (JCPDS No. 29-0497) [31]. The XPS pattern shown in Figure S2(A) (Supporting Information) presents the P 2p, Co 2p and Ni 2p peaks, also verifying the successful preparation of CoP/NF. To be specific, peak deconvolution of the Co 2p XPS provides the two remarkable CoP $2p_{3/2}$ and CoP $2p_{1/2}$ peaks at 781.5 and 797.7 eV, respectively (B). CoO $2p_{3/2}$ and CoO $2p_{1/2}$ peaks are also observed due to the incomplete phosphorization process [32]. For the high-resolution P 2p XPS pattern (C), a doublet situated at 128.9 and 129.8 eV correspond to the P $2p_{3/2}$ and P $2p_{1/2}$ lines, respectively. Another peak at 132.1 eV can be attributed to the oxidized phosphate species [33]. All the above results verify the successful fabrication of the CoP nanosheet array on Ni foam.

3.2. Characteristics of the monolithic CoP/NF peroxidase mimic

(Please insert Figure 2 here)

Figure 2. (A) presents the photograph of the monolithic CoP/NF peroxidase mimic used in our study; (B) shows the time-dependent absorbance changes of different reaction systems. In these systems, 0.05 mL H_2O_2 stock solution (9.8 M), 0.05 mL TMB stock solution (8 mM), 2.9 mL NaAc-HAc buffer (0.2 M, pH 4) and a piece of 1 cm×1 cm CoP/NF ($Co(OH)_2$/NF or NF) were mixed for reaction; (C) depicts the time-dependent absorbance changes of the H_2O_2+TMB+CoP/NF system in which the CoP/NF nanozyme was put into and taken out from the solution optionally with a tiny pair of tweezers; (D) tests the absorbance changes after the CoP/NF nanozyme was finally taken out from the solution in (C).

Different from the previous cases in which transition metal phosphides were

utilized as an electrocatalyst for hydrogen or oxygen evolution [26, 34, 35], we investigated the peroxidase-like properties of the fabricated CoP/NF. As shown in Figure 2(A), the integrated CoP/NF with a size of 1 cm×1 cm or 5 mm×5 mm was used as a monolithic nanozyme in this research. It is able to trigger the color reaction of TMB in the presence of H_2O_2. This color reaction is generally known as the oxidation of colorless TMB catalyzed by hydroxyl radicals from H_2O_2 decomposition into a blue-green TMBox [36, 37]. When anyone of TMB, H_2O_2 and CoP/NF is in the absence, no color reaction occurs (Figure S3, Supporting Information). These results demonstrate the intrinsic peroxidase-like activity of CoP/NF.

In comparison with the $Co(OH)_2$/NF precursor, the prepared CoP/NF exhibits much higher activity to induce the TMB color reaction. As depicted in Figure 2(B), when NF is utilized instead of the CoP/NF peroxidase mimic, no color change is observed, indicating that the NF support has no peroxidase-like activity. With respect to $Co(OH)_2$/NF, a slow increase of the absorbance at 652 nm upon time is found, suggesting that the $Co(OH)_2$/NF precursor also exhibits a certain peroxidase activity. After phosphorization, the resulting CoP/NF results in a rapid increase of the absorbance. This result demonstrates the significantly enhanced peroxidase activity of CoP/NF compared to $Co(OH)_2$/NF.

Different from previously reported nanozymes dispersed in solutions [24], the CoP/NF peroxidase mimic proposed here is a bulk one. Therefore, the monolithic CoP/NF nanozyme can be put into and taken out from reaction systems expediently and promptly with only a tiny pair of tweezers (not like the dispersed nanozyme case

in which complicated centrifugation or magnetic separation is required). To verify this feature, we recorded the time-dependent absorbance changes of the H_2O_2+TMB+CoP/NF system in which the CoP/NF nanozyme was put into and taken out from the solution optionally with tweezers. As presented in Figure 2(C), when the CoP/NF nanozyme is first put into the solution, the catalytic reaction starts to occur, resulting in a rapid increase of the absorbance. When the nanozyme is taken out randomly with a pair of tweezers, the catalytic process of H_2O_2 to hydroxyl radicals is paused, leading to the stop of the TMB oxidation. As a result, no obvious increase of the absorbance is observed during the pause stage. When the CoP/NF is put into the solution again, the color reaction of TMB is reinstated, resulting in the further increase of the absorbance at 652 nm. This phenomenon suggests that the monolithic CoP/NF nanozyme can be used for on-demand detection.

Given that TMB is the most sensitive chromogen for peroxidase with low background interference [38], it is usually employed as the H_2O_2-mediated reaction substrate. Nonetheless, the TMBox species originating from the initial oxidation of TMB is not stable enough. Hence, H_2SO_4 as a termination agent is generally added into the reaction media to stabilize the color [38, 39]. In our case, no strong acid is required to terminate the reaction, because the monolithic CoP/NF peroxidase mimic can be taken out conveniently with tweezers to stop the catalytic process. To verify this characteristic, we further recorded the absorbance changes after the CoP/NF nanozyme was finally taken out from the reaction solution in Figure 2(C). No remarkable change of the absorbance at 652 nm is found within nearly an hour (D).

Particularly, the relative standard deviation (RSD) of the absorbance recorded within the initial 15 min (this time period is supposed to be much enough for optical measurements) is less than 1%, demonstrating the good stability of the reaction media after the monolithic CoP/NF is taken out. This result confirms that no reaction termination agent or stabilizer is required in our system.

Like natural peroxidase, the catalytic activity of the CoP/NF peroxidase mimic is also affected by reaction environments. As depicted in Figure S4 (Supporting Information), the absorbance at 652 nm increases with the increasing TMB content in the reaction solution until a saturation phenomenon appears. What should be pointed out is that the reaction media starts to be turbid when the TMB concentration is higher than 0.13 mM. This is due to the low dissolubility of TMB in aqueous phase. In addition, a volcano-type dependency of the CoP/NF activity toward both the buffer pH (Figure S5, Supporting Information) and the incubation temperature (Figure S6, Supporting Information) is observed. As a result, the buffer with an optimized pH 4 and the best incubation temperature of 30□ was used in the following measurements.

The peroxidase activity of CoP/NF was further evaluated by standard steady-state kinetics measurements. As shown in Figure S7 (Supporting Information), typical Michaelis-Menten catalytic behaviors toward both TMB (A) and H_2O_2 (B) are observed. The apparent K_m values of the CoP/NF nanozyme for TMB and H_2O_2 are calculated to be 0.54 mM and 4.90 mM, respectively. The K_m values measured in natural horseradish peroxidase (HRP) are 0.38 mM and 4.53 mM, respectively [19]. These data demonstrate that the monolithic peroxidase mimic has equivalent affinities

toward the two substrates in comparison with HRP. Furthermore, the prepared monolithic peroxidase mimic possesses higher affinities (with lower K_m values) to the both substrates in comparison to a majority of previously reported peroxidase mimics (Table S1, Supporting Information), indicating the favorable catalytic activity of CoP/NF.

(Please insert Figure 3 here)

Figure 3. The robustness of the CoP/NF nanozyme against (A) harsh pH and (B) temperature. In (A), the CoP/NF peroxidase mimic was first incubated in 0.1 M NaAc-HAc solutions with different pH values for 2 h and then its activity was measured under standard conditions. In (B), the CoP/NF peroxidase mimic was first incubated at different temperatures for 2 h and then its activity was measured; (C) shows the absorbance of reaction systems in which the same piece of CoP/NF was reused repeatedly.

In comparison with natural bio-enzymes, one of the most remarkable merits of nanozymes is their stronger resistance against harsh environments. To check this, we first incubated the CoP/NF nanozyme in solutions with various pH values or at different temperatures for 2 h, and then measured its activity under standard conditions. Our previous studies have revealed that HRP exhibits high activity only in neutral media [16, 19]. With pH decreases or increases, its activity is sharply reduced, and no activity is found in strong acid solutions. With regard to temperature, the activity of HRP rapidly decreases when the incubation temperature exceeds 45□. In contrast, as depicted in Figure 3(A), the CoP/NF nanozyme reported here exhibits no

remarkable change in activity when it is incubated in buffers with a wide range of pH from 2 to 14. Its activity also has no notable change upon temperature (B). These results demonstrate the excellent robustness of the CoP/NF peroxidase mimic.

Since the active CoP nanosheet arrays are integrated on the bulk NF substrate, the resulting CoP/NF nanozyme can be easily recycled and reused. Figure 3(C) compares the absorbances recorded in twelve measurements in which the same piece of CoP/NF was utilized. No difference of these absorbances is observed, resulting in a RSD of 1.6%. This result confirms the good recyclability of the fabricated CoP/NF nanozyme.

As the TMB color reaction originates from a H_2O_2-mediated peroxidase reaction, it can be employed to detect the H_2O_2 substrate. As shown in Figure S8 (Supporting Information), the absorption peak increases along with the increasing amount of H_2O_2 in solutions (A). A rapid linear increase in the absorbance at 652 nm is observed in the H_2O_2 concentration range of 0.032~1.2 mM (R^2 = 0.999). When more H_2O_2 is added, the absorbance further increases mildly in the content scope of 1.5~490 mM (R^2 = 0.989) until a common saturation phenomenon appears. This result demonstrates the feasibility of H_2O_2 detection.

3.3.The TMB color reaction can be suppressed by UA selectively

(Please insert Figure 4 here)

Figure4. (A) compares typical absorption profiles of the H_2O_2+TMB+CoP/NF system with/without UA added simultaneously; (B) illustrates the reaction process in (A); (C) compares typical absorption profiles of the H_2O_2+TMB+CoP/NF system with/without adding UA into the solution after reaction; (D) illustrates the reaction process in (C).

It is interestingly found that UA can selectively suppress the TMB color reaction. As demonstrated in Figure 4(A), an obvious color change (from colorless to blue-green) of the solution is observed in the H_2O_2+TMB+CoP/NF system. When H_2O_2, TMB, CoP/NF and UA are simultaneously added into the NaAc-HAc buffer, no color change of the reaction media is found. This result reveals that the presence of UA is able to suppress the TMB color reaction. The reaction process is illustrated in (B). The possible reasons why the UA species can suppress the TMB color reaction are preliminarily deduced as follows: (1) as the activity of nanozymes highly depends on their surface properties [24], the UA additive may be adsorbed on the CoP/NF surface and inhibit its peroxidase activity; (2) UA may exhaust the hydroxyl radicals generated from H_2O_2 decomposition, thus blocking the TMB oxidation reaction; (3) the UA species may have the capacity to reduce the colored TMBox to colorless TMB again. To find out the specific mechanism, we further carried out a group of experiments: H_2O_2, TMB and CoP/NF were first added into the buffer to trigger the TMB color reaction; after reaction for 35 min, the solution exhibits a distinct blue-green color; the UA species was then added into the media. As depicted in (C), the added UA induces the decolorization of the media. This phenomenon reveals that the suppression of the TMB color reaction originates from the reduction of the blue-green TMBox to colorless TMB again by UA, as illustrated in (D).

3.4.Colorimetric biosensing of UA

(Please insert Figure 5 here)

Figure 5. (A) depicts typical absorption profiles for UA detection using the developed

biosensor; (B) shows the dependency of the absorbance at 652 nm on the UA concentration. The inset presents the photograph of reaction systems in which different amounts of UA were added; (C) shows the linear relationship between the absorbance and the UA concentration; (D) compares the decreased absorbance induced by various species (800 μM UA, 800 μM AA, 8 mM urea, 8 mM Trig, 8 mM Chol or 8 mM Glu).

According to the above finding, a new biosensor with no use of any natural enzyme was developed for the colorimetric detection of UA. The biosensor works based on the suppression of the TMB color reaction (which easily occurs in the presence of the CoP/NF peroxidase mimic and H_2O_2) by UA specifically. As demonstrated by Figure 5(A), the absorption peak decreases along with the increasing UA concentration. Surprisingly, a very small amount of UA can induce the rapid decrease of the absorbance at 652 nm (B). When more UA is added into the reaction solution, the decline rate of the absorbance gradually slows down until a saturation state appears. It is found that the dependency of the absorbance on the UA concentration from 1 to 200 μM can be well described by an equation of $Y = 0.038 + 0.351*0.965^X$ (Y is the absorbance at 652 nm, and X is the UA concentration (μM), $R^2 = 0.991$). The limit of detection (LOD) is down to 1.0 μM. As depicted in (C), the absorbance is also linear to the analyte concentration in the range of 1~30 μM ($R^2 = 0.990$). Table S2 (Supporting Information) compares the analytical performance of previously reported biosensors with ours. Both the detection range and the LOD of our biosensor are comparable or even better. More attractively, our biosensor can work with no use of

any natural enzyme including the uricase, and this characteristic endows the developed biosensor with favorable reproducibility and stability. As a result, six measurements of 0.1 mM UA within 45 days using the same piece of CoP/NF lead to a RSD of 2.9%. When the CoP/NF peroxidase mimic from three preparation batches is employed, nine measurements result in a RSD of 2.3%.

To investigate the specificity of the developed biosensor, several species commonly existing in blood and urine were checked. Figure 5(D) compares the decreased absorbance of 800 μM UA, 800 μM AA, 8 mM urea, 8 mM Glu, 8 mM Chol and 8 mM Trig. Obviously, only UA can induce the suppression of the TMB color reaction, demonstrating the good selectivity of the fabricated biosensor for UA detection.

3.5. Application of the developed biosensor for UA analysis in real samples

To investigate the practical application ability of the developed UA biosensor, we applied it to detect the target in clinical samples. Three human serum and two urine samples from the hospital were employed for analysis. Since the content of UA in serum is generally among 100~500 μM and the detection range of our biosensor is 1~200 μM, so the serum samples can be detected directly by adding 100 μL of a serum sample into the reaction system with a total volume of 3 mL. Considering that the UA level in urine may be beyond the detection scope, a dilution process was performed before measurements. The results obtained by our biosensor are compared with the clinical data, as listed in Table 1. For all serum samples, the UA levels detected by our developed biosensor are in good agreement with the clinical results, resulting in the relative error (RE) less than ±5%. For all urine samples, the recovery

values are among 99%~107%. The excellent reliability for UA detection in these clinical samples verifies the good practicability of our biosensor. Additionally, good repeatability of the UA colorimetric biosensor is also acquired during practical sample measurements.

Table 1. The contents of UA in human serum and urine detected by the clinical method and our developed biosensor.

Sample[a]		Clinical (μM)	Measured (μM)[b]	RE (%)	Recovery (%)
Serum 1		195.9	187.3±10.6	-4.4	—
Serum 2		484.3	506.5±15.1	+4.6	—
Serum 3		192.1	188.0±5.6	-2.1	—
	—	—	50.8±4.2	—	—
Urine 1	+20 μM	—	72.1±3.4	—	106.5
	+50 μM	—	102.1±10.1	—	102.6
	—	—	27.6±3.3	—	—
Urine 2	+20 μM	—	47.9±5.8	—	101.5
	+50 μM	—	77.4±1.9	—	99.6

[a] The serum samples were de-proteined before detection, and the urine samples were diluted 2.67 times with 0.1 M phosphate buffer (pH 8.5) before measurements

[b] Each sample was detected repeatedly for three times

4. Conclusions

In summary, CoP nanosheet arrays integrated on NF surface have been fabricated as a monolithic nanozyme, exhibiting significantly enhanced peroxidase-like activity

to trigger the color reaction of TMB with the participation of H_2O_2. Different from previous nanozymes dispersed in solutions, the monolithic CoP/NF can be put into or taken out from systems promptly with only tweezers to start or stop the catalytic reaction optionally, which enables the on-demand detection. This feature also avoids the use of strong acid as the reaction terminating agent. It is found that the color reaction of TMB can be suppressed by UA selectively. Hence, a new UA colorimetric biosensor has been successfully developed based on this finding. The UA biosensor requires for neither natural peroxidase nor uricase, providing good repeatability and excellent stability against environments. It also offers favorable reliability for the biosensing of UA in clinical samples. Taken together, the advantages of no natural enzyme and termination agent, on-demand analysis, good recyclability of nanozyme, excellent analytical performance and visual detection enable the developed biosensor to be a promising tool for UA detection.

Acknowledgements

This research was supported by the National Natural Science Foundation of China (Nos. 21605061 and 31601549), the Natural Science Foundation of Jiangsu Province (No. BK20160489), the Natural Science Fund for Colleges and Universities in Jiangsu Province (No. 16KJB150009), the Postdoctoral Fund of China (No. 2016M600365), the Postdoctoral Fund of Jiangsu Province (No. 1601015B), and the Open Fund from the Shanghai Key Laboratory of Functional Materials Chemistry (No. SKLFMC201601). We also thank the financial supports from the Youth Talent Cultivation Plan of Jiangsu University and the Open Funding Project of the State Key

Laboratory of Bioreactor Engineering.

References

[1] G.F. Falasca, Metabolic diseases: gout, Clin. Dermatol. 24 (2006) 498-508.

[2] W.L. Nyhan, Disorders of purine and pyrimidine metabolism, Mol. Genet. Metab. 86 (2005) 25-33.

[3] W.L. Nyhan, The Lesch-Nyhan syndrome, Annu. Rev. Med. 24 (1973) 41-60.

[4] Y.C. Luo, J.S. Do, C.C. Liu, An amperometric uric acid biosensor based on modified Ir-C electrode, Biosens. Bioelectron. 22 (2006) 482-488.

[5] L. Liddle, J.E. Seegmiller, L. Laster, The enzymatic spectrophotometric method for determination of uric acid, J. Lab. Clin. Med. 54 (1959) 903-913.

[6] N. Kageyama, A direct colorimetric determination of uric acid in serum and urine with uricase-catalase system, Clin. Chim. Acta 31 (1971) 421-426.

[7] P. Fossati, L. Prencipe, G. Berti, Use of 3,5-dichloro-2-hydroxybenzenesulfonic acid/4-aminophenazone chromogenic system in direct enzymic assay of uric acid in serum and urine, Clin. Chem. 26 (1980) 227-231.

[8] D. Martinez-Pérez, M.L. Ferrer, C.R. Mateo, A reagent less fluorescent sol-gel biosensor for uric acid detection in biological fluids, Anal. Biochem. 322 (2003) 238-242.

[9] N.E. Azmi, N.I. Ramli, J. Abdullah, M.A.A. Hamid, H. Sidek, S.A. Rahman, N. Ariffin, N.A. Yusof, A simple and sensitive fluorescence based biosensor for the determination of uric acid using H_2O_2-sensitive quantum dots/dual enzymes, Biosens. Bioelectron. 67 (2015) 129-133.

[10] P.E. Erden, E. Kiliç, A review of enzymatic uric acid biosensors based on amperometric detection, Talanta 107 (2013) 312-323.

[11] L.Z. Gao, J. Zhuang, L. Nie, J.B. Zhang, Y. Zhang, N. Gu, T.H. Wang, J. Feng, D.L. Yang, S. Perrett, X.Y. Yan, Intrinsic peroxidase-like activity of ferromagnetic nanoparticles, Nat. Nanotechnol. 2 (2007) 577-583.

[12] H. Wei, E.K. Wang, Nanomaterials with enzyme-like characteristics (nanozymes): next-generation artificial enzymes, Chem. Soc. Rev. 42 (2013) 6060-6093.

[13] R. Ragg, M.N. Tahir, W. Tremel, Solids go bio: inorganic nanoparticles as enzyme mimics, Eur. J. Inorg. Chem. 2016 (2016) 1906-1915.

[14] K. Korschelt, R. Ragg, C.S. Metzger, M. Kluenker, M. Oster, B. Barton, M. Panthöfer, D. Strand, U. Kolb, M. Mondeshki, S. Strand, J. Brieger, M.N. Tahir, W. Tremel, Glycine-functionalized copper(II) hydroxide nanoparticles with high intrinsic superoxide dismutase activity, Nanoscale 9 (2017) 3952-3960.

[15] A.A. Vernekar, T. Das, S. Ghosh, G. Mugesh, A remarkably efficient $MnFe_2O_4$-based oxidase nanozyme, Chem. – Asian J. 11 (2016) 72-76.

[16] Y.F. He, X.H. Niu, L.B. Shi, H.L. Zhao, X. Li, W.C. Zhang, J.M. Pan, X.F. Zhang, Y.S. Yan, M.B. Lan, Photometric determination of free cholesterol via cholesterol oxidase and carbon nanotube supported Prussian blue as a peroxidase mimic, Microchim. Acta 184 (2017) 2181-2189.

[17] E. Kuah, S. Toh, J. Yee, Q. Ma, Z.Q. Gao, Enzyme mimics: advances and applications, Chem. – Eur. J. 22 (2016) 8404-8430.

[18] M. Nasir, M.H. Nawaz, U. Latif, M. Yaqub, A. Hayat, A. Rahim, An overview on enzyme-mimicking nanomaterials for use in electrochemical and optical assays, Microchim. Acta 184 (2017) 323-342.

[19] X.H. Niu, Y.F. He, J.M. Pan, X. Li, F.X. Qiu, Y.S. Yan, L.B. Shi, H.L. Zhao, M.B. Lan, Uncapped nanobranch-based CuS clews used as an efficient peroxidase mimic enable the visual detection of hydrogen peroxide and glucose with fast response, Anal. Chim. Acta 947 (2016) 42-49.

[20] J.Y. Lu, Y.H. Xiong, C.J. Liao, F.G. Ye, Colorimetric detection of uric acid in human urine and serum based on peroxidase mimetic activity of MIL-53(Fe), Anal. Methods 7 (2015) 9894-9899.

[21] A.J. Fang, Q.Q. Wu, Q.J. Lu, H.Y. Chen, H.T. Li, M.L. Liu, Y.Y. Zhang, S.Z. Yao, Up-conversion ratiometric fluorescence and colorimetric dual-readout assay for uric acid, Biosens. Bioelectron. 86 (2016) 664-670.

[22] Q.Q. Zhuang, Z.H. Lin, Y.C. Jiang, H.H. Deng, S.B. He, L.T. Su, X.Q. Shi, W. Chen, Peroxidase-like activity of nanocrystalline cobalt selenide and its application for uric acid detection, Int. J. Nanomedicine 12 (2017) 3295-3302.

[23] H.F. Lu, J.Y. Li, M.M. Zhang, D. Wu, Q.L. Zhang, A highly selective and sensitive colorimetric uric acid biosensor based on Cu(II)-catalyzed oxidation of 3,3′,5,5′-tetramethylbenzidine, Sens. Actuators, B 244 (2017) 77-83.

[24] B.W. Liu, J.W. Liu, Surface modification of nanozymes, Nano Res. 10 (2017) 1125-1148.

[25] X.H. Niu, H.L. Zhao, M.B. Lan, Palladium deposits spontaneously grown on

nickel foam for electrocatalyzing methanol oxidation: effect of precursors, J. Power Sources 306 (2016) 361-368.

[26] X.P. Zhang, Y.J. Han, L. Huang, S.J. Dong, 3D graphene aerogels decorated with cobalt phosphide nanoparticles as electrocatalysts for the hydrogen evolution reaction, ChemSusChem 9 (2016) 3049-3053.

[27] W.Y. Yuan, X.Y. Wang, X.L. Zhong, C.M. Li, CoP nanoparticles in situ grown in three-dimensional hierarchical nanoporous carbons as superior electrocatalysts for hydrogen evolution, ACS Appl. Mater. Interfaces 8 (2016) 20720-20729.

[28] Q. Li, J.J. Ma, H.J. Wang, X. Yang, R. Yuan, Y.Q. Chai, Interconnected Ni_2P nanorods grown on nickel foam for binder free lithium ion batteries, Electrochim. Acta 213 (2016) 201-206.

[29] T. Chen, D.N. Liu, W.B. Lu, K.Y. Wang, G. Du, A.M. Asiri, X.P. Sun, Three-dimensional Ni_2P nanoarray: an efficient catalyst electrode for sensitive and selective nonenzymatic glucose sensing with high specificity, Anal. Chem. 88 (2016) 7885-7889.

[30] L. Cui, Y.H. Xu, L. Niu, W.R. Yang, J.Q. Liu, Monolithically integrated CoP nanowires array: an on/off switch for effective on-demand hydrogen generation via hydrolysis of $NaBH_4$ and NH_3BH_3, Nano Res. 10 (2017) 595-604.

[31] J.Q. Tian, Q. Liu, A.M. Asiri, X.P. Sun, Self-supported nanoporous cobalt phosphide nanowire arrays: an efficient 3D hydrogen-evolving cathode over the wide range of pH 0-14, J. Am. Chem. Soc. 136 (2014) 7587-90.

[32] J.F. Chang, Y. Xiao, M.L. Xiao, J.J. Ge, C.P. Liu, W. Xing, Surface oxidized

cobalt-phosphide nanorods as an advanced oxygen evolution catalyst in alkaline solution, ACS Catal. 5 (2015) 6874-6878.

[33] Y.P. Zhu, Y.P. Liu, T.Z. Ren, Z.Y. Yuan, Self-supported cobalt phosphide mesoporous nanorod arrays: a flexible and bifunctional electrode for highly active electrocatalytic water reduction and oxidation, Adv. Funct. Mater. 25 (2015) 7337-7347.

[34] A. Mendoza-Garcia, D. Su, S.H. Sun, Sea urchin-like cobalt-iron phosphide as an active catalyst for oxygen evolution reaction, Nanoscale 8 (2016) 3244-3247.

[35] D.H. Xiong, X.G. Wang, W. Li, L.F. Liu, Facile synthesis of iron phosphide nanorods for efficient and durable electrochemical oxygen evolution, Chem. Commun. 52 (2016) 8711-8714.

[36] J.X. Xie, H.Y. Cao, H. Jiang, Y.J. Chen, W.B. Shi, H.Z. Zheng, Y.M. Huang, Co_3O_4-reduced graphene oxide nanocomposite as an effective peroxidase mimetic and its application in visual biosensing of glucose, Anal. Chim. Acta 796 (2013) 92-100.

[37] N.R. Nirala, S. Pandey, A. Bansal, V.K. Singh, B. Mukherjee, P.S. Saxena, A. Srivastava, Different shades of cholesterol: gold nanoparticles supported on MoS_2nanoribbons for enhanced colorimetric sensing of free cholesterol, Biosens. Bioelectron. 74 (2015) 207-213.

[38] P. Fanjul-Bolado, M.B. Gonzalez-Garcia, A. Costa-Garcia, Amperometric detection in TMB/HRP-based assays, Anal. Bioanal. Chem. 382 (2005) 297-302.

[39] B.Y.C. Ng, E.J.H. Wee, N.P. West, M. Trau, Naked-eye colorimetric and electrochemical detection of Mycobacterium tuberculosis—toward rapid screening for

1 active case finding, ACS Sens. 1 (2016) 173-178.

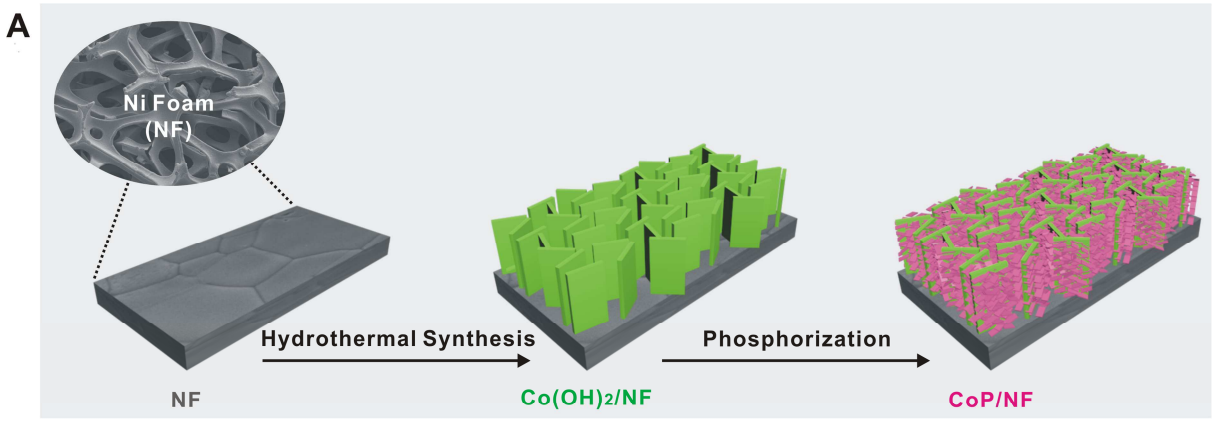

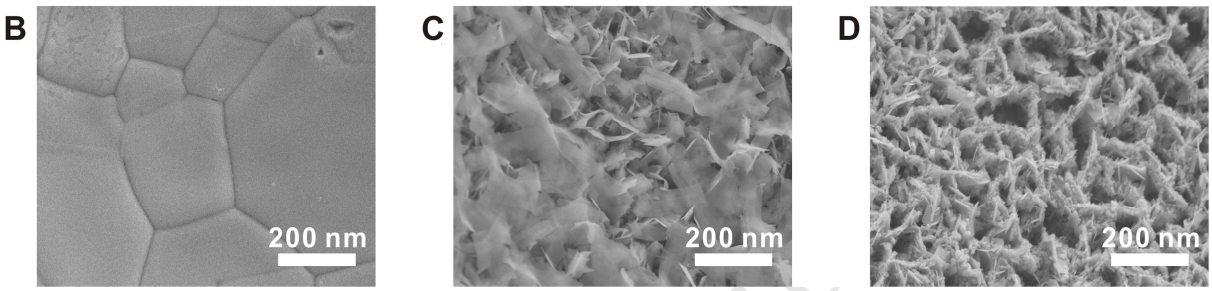

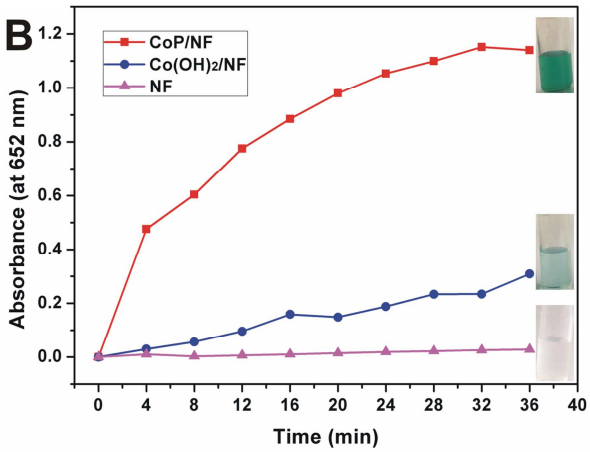

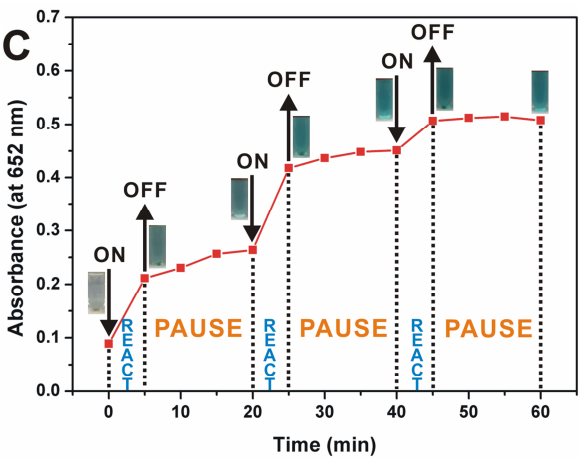

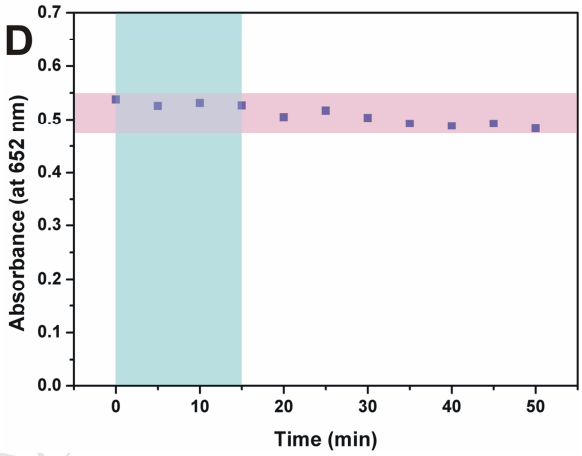

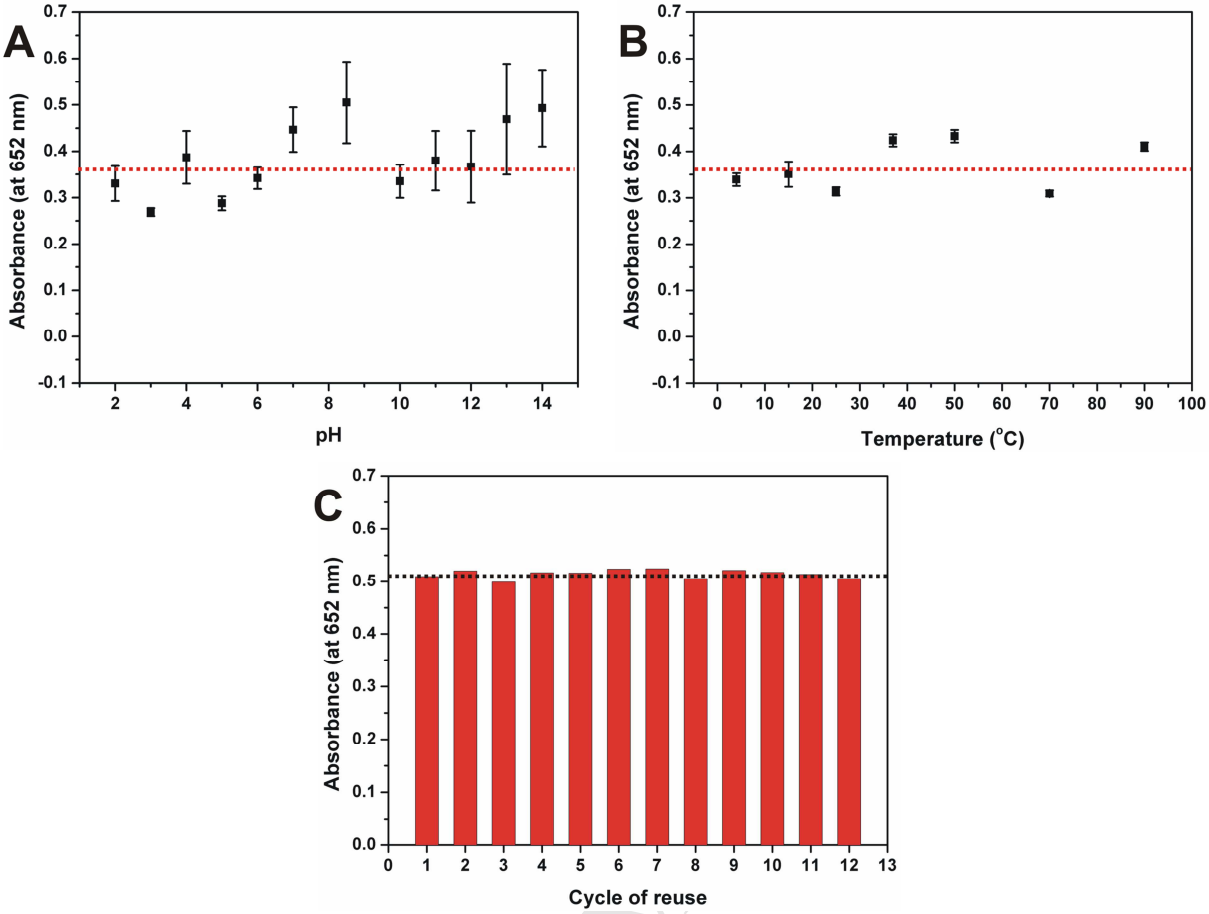

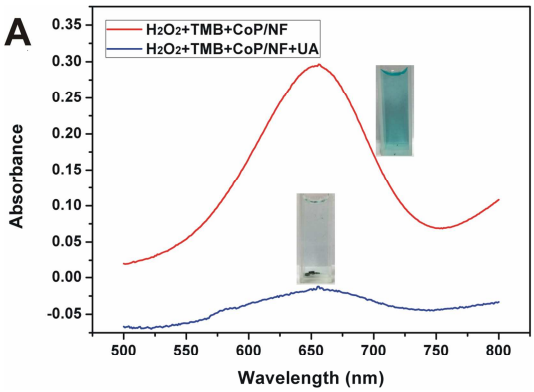

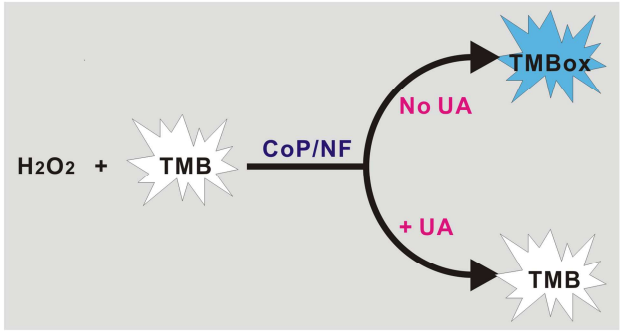

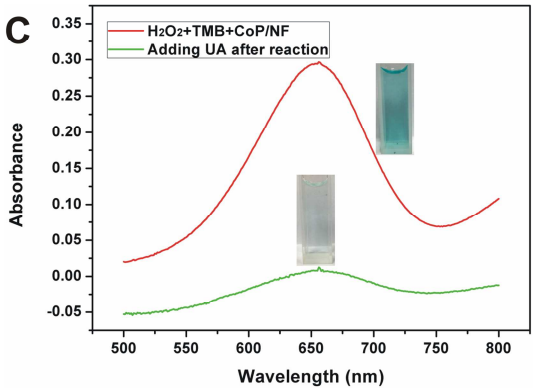

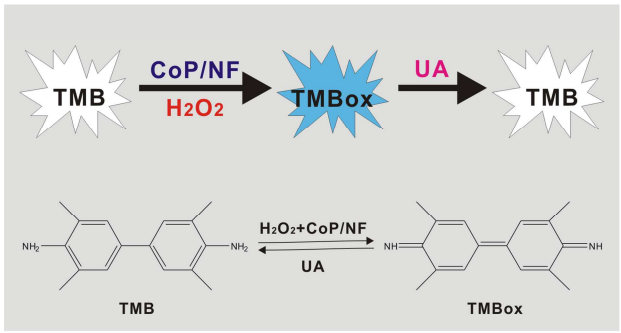

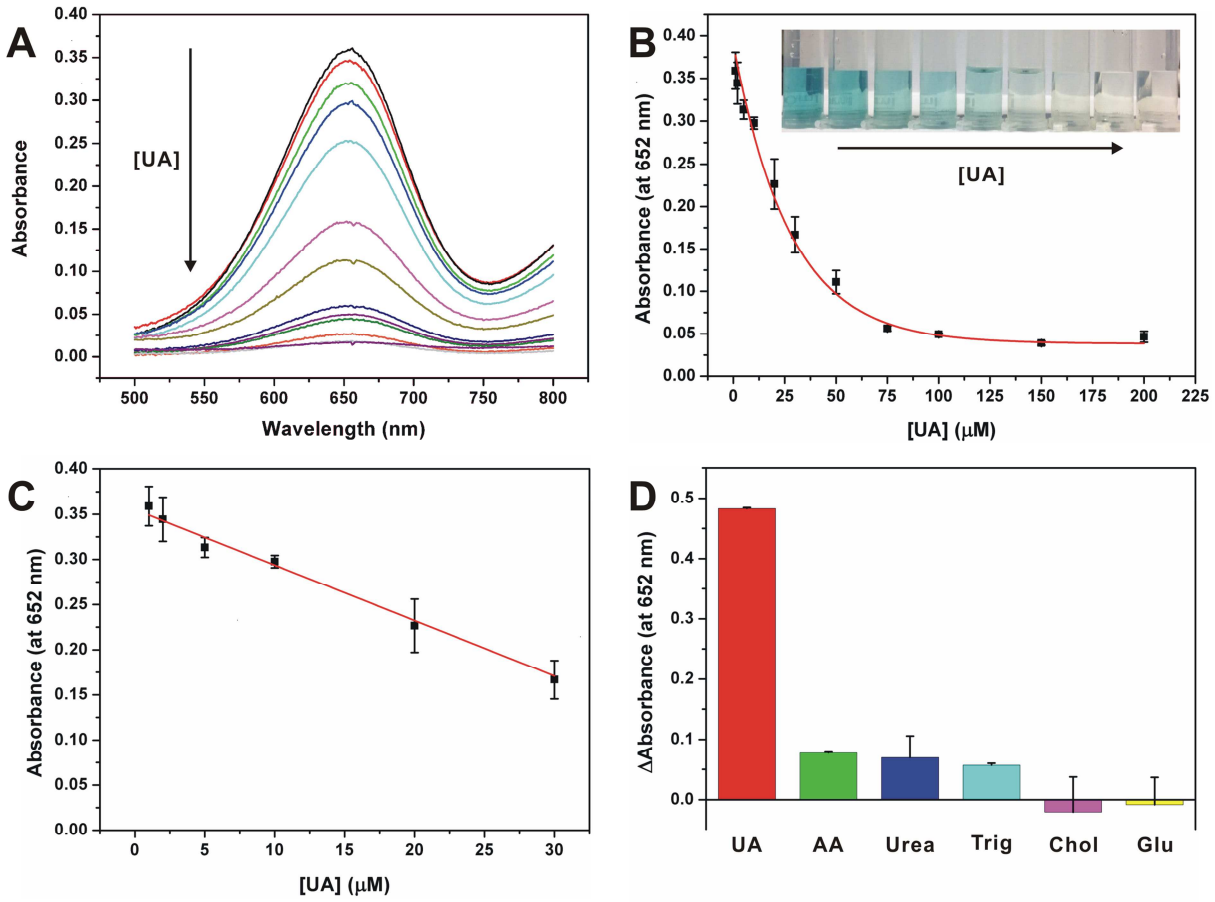

Highlights

- Integrated CoP nanosheet arrays as a monolithic peroxidase mimic;
- Easy to be manipulated by only tweezers to realize on-demand analysis;
- The TMB color reaction induced by H_2O_2 and CoP/NF is suppressed by UA selectively;
- A novel colorimetric biosensor for natural enzyme-free detection of UA.